Pure Appl. Geophys.

https://doi.org/10.1007/s00024-024-03559-0

Pure and Applied Geophysics

Prediction of Precipitation-Temperature Data and Drought Assessment of Turkey with Stochastic Time Series Models

Ahmet Iyad Ceyhunlu[1] and Gokmen Ceribasi[2]

Abstract—Throughout the geological history of Earth, there have been many changes in the climate system due to natural and external factors. In the past, it can be said that changes in climate were caused by natural causes, while today they are largely caused by human activities. Turkey is among the countries that will be affected by climate change. Therefore, In this study, a stochastic time series model was constructed to forecast the precipitation and temperature data of Turkey between 2020 and 2050. Seasonal Autoregressive Integrated Moving Average models were used to take into account the relationship between the data and seasonality factors. In addition, the most appropriate model for each station was established separately. The accuracy of the predicted data was tested by correlation test (r) and root mean square error (RMSE) test. As a result of the study, the average r value for temperature data was 99% and RMSE value was calculated as 1.46. For precipitation data, the average r value was calculated as 66% and RMSE value as 34.6. In addition, in this study, drought models for Turkey until 2050 were established and spatial and temporal evaluation of these models were made. These models were obtained by analyzing the data of uniformly distributed stations over Turkey between 1990 and 2050 with standard precipitation evapotranspiration index (SPEI). Different time scales ($SPEI_3$, $SPEI_6$, $SPEI_9$ and $SPEI_{12}$) were used in drought analysis. As a result of this study, drought return interval maps of Turkey and drought maps between 1990 and 2050 were created.

Keywords: Climate Change, Precipitation, Temperature, Stochastic time series, Drought, Turkey.

1. Introduction

Stochastic time series models (STSM) are models in which statistical methods are used to create models and forecasts by examining the changes in random variables over time. STSM refers to the sequence of data measured within a time interval. Traffic density, sales figures, stocks, stock market data, energy production data, rainfall and temperature data can be given as examples of the data of this model (Al-Najjar et. al., 2020). Stochastic time series models have been widely used in recent times because they can be used in many different fields and because of their precise results. For example, they are used to analyze time-varying data in fields such as economics, finance, meteorology, social sciences, engineering and epidemiology. Analyzing these series can provide a lot of useful information, such as predicting future values, identifying trends, identifying cycles and making forecasts (Al-Najjar et. al., 2020).

Many statistical methods and models are available for stochastic time series analysis. For example, moving average (MA), autoregressive integrated moving average (ARIMA), autoregressive moving average (ARMA), autoregressive time series (AR), seasonal autoregressive integrated moving average predictor (SARIMA), long memory models and generalized autoregressive conditional heteroskedastic (GARCH) models are frequently used. Stochastic time series analysis has many applications such as forecasting future events and assessing risks. Stochastic time series models were first proposed by Box and Jenkins in 1976 (Box & Jenkins, 1976). In their study, Box and Jenkins first proposed the theorem and methodology called ARIMA. In the literature, many studies have been conducted with these methods in different fields of study. Mishra et al. (2005) estimated the drought of Kansabati River basin in India using ARIMA and SARIMA models. They used standardized precipitation index (SPI) for

[1] Department of Civil Engineering, Sakarya University of Applied Sciences, Faculty of Technology, Sakarya, Turkey. E-mail: ahmetceyhunlu@subu.edu.tr

[2] Department of Civil Engineering, Sakarya University of Applied Sciences, Faculty of Technology, Sakarya, Turkey. E-mail: gceribasi@subu.edu.tr

Published online: 19 August 2024

drought analysis. As a result of the study, they suggested that the predicted drought value decreased with the increase in the supply period, but they obtained good results for forecasts up to two months. Chen et al. (2007) proposed a hybrid methodology combining SARIMA and support vector machines (SVM) models to forecast seasonal time series data. They used Taiwan machinery industry production data in the study. As a result of the study, they concluded that the mean squared error and absolute percentage error values of the proposed hybrid model were the lowest. Kam et al. (2010) defined the number of patients coming to the emergency room as the dependent variable and data such as day of the week, holidays, air temperature, precipitation, etc. as independent variables. They aimed to create a multivariate SARIMA model by considering additional factors that may affect the analyzed time series. The study used historical daily patient counts to assess the applicability of time series analysis. The researchers used SARIMA model to analyze the data. They argued that SARIMA model enables more accurate forecasts by taking into account seasonal components and trends in the data. The study shows that SARIMA model is effective in forecasting daily patient counts. The model successfully captured time series features such as seasonal fluctuations and trends and was able to make forecasts with high accuracy. They concluded that the multivariate SARIMA model is more reliable and the most appropriate model for predicting the number of patients per day. Durdu (2010) aimed to obtain seasonal and non-seasonal forecasts of SPI data with linear stochastic time series. Büyük Menderes Basin of Turkey was used as the study area in the study. He suggested that the drought data obtained as a result of the study are in good agreement with the actual data. Modarres et al. (2013) modeled the variance in the residuals of SARIMA models using GARCH model. Djerbouai et al. (2016) aim to predict drought in the Algerois Basin in Algeria with traditional stochastic models such as artificial neural networks (ANN), ARIMA and SARIMA. In their study, they determined the best model by analyzing NSE, RMSE and MAE. Aghelpour et al. (2019) argue that the accuracy of long-term temperature forecasts plays a crucial role in informing environmental policies related to global climate change. In this study, they compared the seasonal autoregressive integrated moving average (SARIMA) stochastic model with the support vector regression (SVR) model and the Firefly optimization algorithm (SVR-FA) model with a combined SVR type. In the study, 75% of the data was used as training data and 25% was used for testing. As a result of the study, it was suggested that the models performed better in extra hot or cold climates. Dabral et al. (2020) used SARIMA models for trend detection in the Umiam region of Meghalaya, India. In the study, they aimed to model and forecast monthly precipitation and temperature time series. The study used different trend analysis methods to identify trends in monthly precipitation, average maximum and minimum temperatures.

Drought is also defined as a natural disaster characterized by a prolonged period of exceptionally low rainfall causing a severe water deficit. It is a climatic phenomenon that has significant negative impacts on the environment, society and economy in many different regions of the world. Local water resources in the regions where drought occurs become unable to meet the demands of people, animals and plants, affecting the lives of all living things (Gultepe et al., 2016, 2019; Gumus, 2023; Hamed et al., 2023; Kao & Govindaraju, 2010; Lotfirad et al., 2022; Mishra et al., 2009; Şen, 1998; Shayeghi et al., 2024). As a result of decreases in precipitation or changes in their intensity, soil moisture decreases. As a result, rivers, lakes and reservoirs dry up, depleting groundwater resources. As a result, agricultural productivity declines, ecosystems are damaged and communities face water scarcity for drinking, irrigation and industrial purposes. Droughts are classified into different types depending on time and area of impact. The main types of this classification are given in Fig. 1 respectively.

While the types of droughts shown in Fig. 1 can persist for weeks or years, prolonged droughts can have the greatest detrimental impacts (Xu et al., 2015). Therefore, the impacts of drought go beyond temporary water scarcity. The negative impacts of drought include food shortages, biodiversity and economic losses due to reductions in agricultural production and increased demand for water from alternative sources. Drought also poses significant

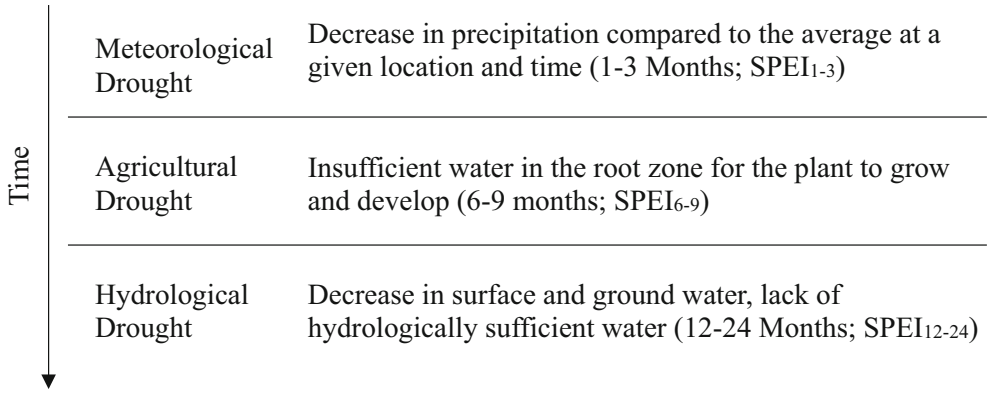

Figure 1
Drought Types Depending on Time

challenges for water management. Developing effective water conservation and allocation strategies is crucial to mitigate the impacts of these challenges.

As a result of scientific studies, it has been suggested that some regions will experience more frequent and severe droughts due to climate change (Guardiola-Claramonte et al., 2011). Increased evaporation rates and variable precipitation regimes brought about by rising global temperatures may increase the probability of droughts and prolong the duration of droughts (Blenkinsop & Fowler, 2007). Recent studies claim that severe droughts have occurred in the last 35 years and that Africa, the Middle East and the Mediterranean countries will be the most affected by these droughts (Bates et al., 2008). Scientists emphasize that the impact of climate change should be taken into account in terms of the management of water resources in regions where drought is experienced (Şen, (2014a). In order to predict the effects of drought and the damage it may cause, accurate scientific methods and observation-based models should be used. Looking at the literature, it is known that the complex structure of drought analysis has been addressed and different indices (indicators) have been designed for this situation. One of these indices is SPI introduced by McKee et al. (1993). Another widely used index is Palmer Drought Severity Index (PDSI). Paulo and Pereira (2008) conducted drought analysis of areas belonging to different regions of the world with SPI and PDSI in their study.

SPI has a simple and straightforward application structure. SPI considers only precipitation data in drought analysis. However, SPI's infrastructure is suitable for the analysis of meteorological, agricultural and hydrological drought periods, which has led to its widespread use (Mishra and Desai, 2005; Doğan et al., 2012). There are also different indices developed for drought analysis. Examples of these are reconnaissance drought index (RDI) and standardized precipitation, evaporation and evapotranspiration index (SPEI). The RDI was introduced in Tsakiris et al. (2007). The RDI calculates drought by considering the ratios of total precipitation, evapotranspiration and potential evaporation. Vicente-Serrano et al. (2010) introduced SPEI. SPEI takes into account the sum of total rainfall, evapotranspiration and potential evaporation. Kao and Govindaraju (2010) developed the joint drought index (JDI) using runoff and rainfall data. In addition to these methods, triple drought index (TDI), multivariate standardized drought index (MSDI) was introduced by Hao and Agha Kouchak (2013) and multivariate drought index (MDI) was introduced by Rajsekhar et al. (2015). In addition, the duration, areal extent, severity and frequency of drought should also be considered in drought analysis (Mishra & Singh, 2010). Because drought is not only caused by low rainfall in a region. At the same time, drought can also be experienced in regions with sudden and heavy rainfall (Şen, 2015a). Therefore, SARIMA models were selected to analyze time series data with

seasonal components in this study. SARIMA models are known for their effectiveness in forecasting climate data, especially those with seasonal and trend components. These models provide highly accurate forecasts by capturing the autocorrelation structure and seasonal trends in time series data. GARCH and Value-at-Risk (VaR) models, which are among the alternative models, do not have the seasonal analysis capabilities of SARIMA. Moreover, SARIMA models have a wide range of applications in the literature and are frequently used in drought and climate change analysis. The advantages of using SARIMA models in this study are their success in capturing seasonal patterns and their computationally less resource-intensive nature. Hence, it is aimed to establish drought models by forecasting meteorological data until 2050 in Turkey and to evaluate these models spatially and temporally in this study. These models will be obtained by analyzing the data of stations uniformly distributed over Turkey between 1990 and 2050 with SPEI. Different time scales (SPEI3, SPEI6, SPEI9 and SPEI12) will be used in drought analysis. In addition, spatial prediction will be made using geographic information systems (GIS) in order to ensure that the drought analysis covers the whole Turkey. As a result of the study, drought return interval maps and drought maps for the years 1990–1999, 2000–2009, 2010–2019, 2020–2029, 2030–2039, 2040–2049 will be created for Turkey.

2. Material and Method

In this study, a stochastic time series model will be established to forecast the precipitation and temperature data of Turkey between 1990 and 2020 until 2050. SARIMA models will be used to take into account the relationship between the data and seasonality factors. In addition, the most appropriate model for each station will be established separately. The steps to be applied in this part of study are given in Fig. 2.

Based on flowchart, meteorological data including precipitation and temperature ratios from various regions of Turkey were collected in the data acquisition phase and the necessary data set for the modeling process will be created. Then, in the time series analysis phase, these data will be analyzed using stochastic time series models and the historical trends and cyclical characteristics of the data will be determined. Third, in the process of defining the model structure, an appropriate time series model structure (e.g. ARIMA or SARIMA) will be selected based on the analysis results and the parameters of the model will be determined. Fourth, in the estimation of model parameters stage, the model will be constructed by estimating the required parameters according to the specified model structure. Fifth, various tests will be performed in the model testing and validation phase to test the model and assess its accuracy. In the sixth stage, future meteorological data will be predicted by time series forecasting and basic data for drought analysis will be obtained. In the seventh stage, drought conditions will be evaluated and drought models will be developed with the predicted data in the process of building drought models. Finally, in the eighth stage, during the production of drought maps of Turkey, the results of drought models will be mapped using geographic information systems (GIS) and the geographical distribution of drought conditions will be visualized. Kriging method, one of the spatial interpolation techniques, will be used to create the maps. This method is used to estimate values from known data points to unknown points, taking into account the spatial dependence between points in a given geographical area. The Kriging method is particularly effective with irregularly spaced data and when variables are spatially correlated. In the process of creating the maps, SPEI values obtained in certain time periods will be used and these values will be estimated spatially across Turkey (Al-Najjar et al., 2020).

2.1. Study Area

In this study, it is aimed to analyze the temperature and precipitation data of Turkey between 1990 and 2020 with SARIMA model and to forecast them prospectively with stochastic time series models. In the study, temperature and precipitation data will be predicted until 2050. For this reason, 37 stations that can best represent Turkey were selected as the study area. The data to be used in study were measured by

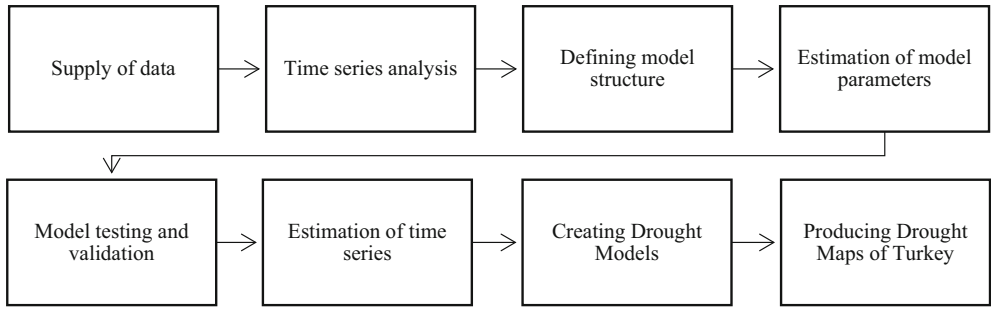

Figure 2
Flowchart of The Study

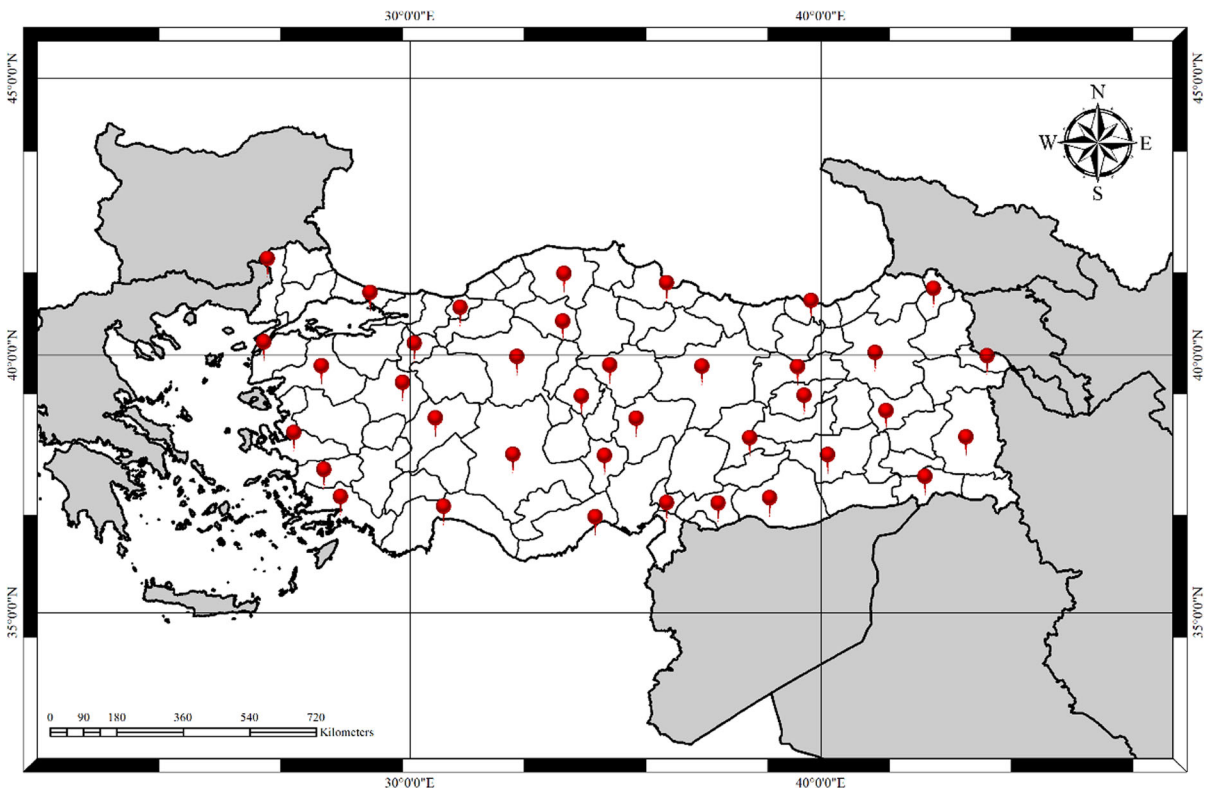

Figure 3
The locations of All Stations Used in The Study on The Map of Turkey

General Directorate of Meteorology (MGM) and obtained from the central station of each province. The map of the study area is given in Fig. 3.

2.2. *Data Forecasting and Analysis*

Between 1990 and 2020, daily total precipitation and daily average temperature data for 81 provincial central stations of Turkey were obtained from MGM. These data obtained from MGM were collected by

Table 1

General Information of Meteorological Stations

Province No	Station Name	Station No	Altitude	Latitude
03	AFYONKARAHISAR	17,190	1013	38°44′16.9"N—30°33′37.4"E
06	ANKARA	17,130	870	39°58′21.9"N—32°51′49.1"E
07	ANTALYA	17,300	43	36°54′22.7"N—30°47′56.4"E
09	AYDIN	17,234	92	37°50′24.9"N—27°50′16.5"E
10	BALIKESIR	17,150	101	39°37′00.0"N—27°55′00.0"E
11	BILECIK	17,120	526	40°08′29.0"N—29°58′38.1"E
17	CANAKKALE	17,112	3	40°08′27.6"N—26°23′57.4"E
18	CANKIRI	17,080	730	40°36′29.4"N—33°36′36.8"E
21	DIYARBAKIR	17,280	674	37°53′50.3"N—40°12′09.7"E
22	EDIRNE	17,050	48	41°40′36.1"N—26°33′03.0"E
24	ERZINCAN	17,094	1214	39°45′08.4"N—39°29′12.6"E
25	ERZURUM	17,096	1893	39°57′10.4"N—41°11′22.9"E
27	GAZIANTEP	17,261	838	37°03′30.6"N—37°21′03.6"E
33	MERSIN	17,340	10	36°46′51.0"N—34°36′11.0"E
34	ISTANBUL	17,061	30	41°08′47.0"N—29°03′00.7"E
35	IZMIR	17,220	10	38°23′40.2"N—27°04′55.6"E
37	KASTAMONU	17,074	800	41°22′15.5"N—33°46′32.2"E
38	KAYSERI	17,196	1071	38°41′13.2"N—35°30′00.0"E
40	KIRSEHIR	17,160	985	39°09′50.2"N—34°09′22.0"E
42	KONYA	17,244	1026	37°59′01.3"N—32°34′26.4"E
43	KUTAHYA	17,155	969	39°25′01.7"N—29°59′20.6"E
44	MALATYA	17,199	972	38°20′12.0"N—38°13′02.4"E
48	MUGLA	17,292	646	37°12′34.2"N—28°22′00.6"E
49	MUS	17,204	1300	38°45′03.3"N—41°30′08.1"E
51	NIGDE	17,250	1208	37°57′30.6"N—34°40′46.2"E
55	SAMSUN	17,030	10	41°20′39.0"N—36°15′23.0"E
58	SIVAS	17,090	1285	39°44′37.2"N—37°00′07.2"E
61	TRABZON	17,038	37	40°59′42.0"N—39°46′58.8"E
62	TUNCELI	17,165	914	39°06′21.0"N—39°32′27.0"E
63	SANLIURFA	17,270	547	37°09′38.9"N—38°47′10.7"E
65	VAN	17,172	1661	38°28′08.9"N—43°20′45.6"E
66	YOZGAT	17,140	1317	39°49′27.6"N—34°48′57.3"E
73	SIRNAK	17,950	377	37°19′53.6"N—42°12′37.3"E
75	ARDAHAN	17,046	1800	41°06′21.9"N—42°42′20.0"E
76	IGDIR	17,100	858	39°55′33.3"N—44°03′13.4"E
80	OSMANIYE	17,355	120	37°06′07.6"N—36°15′14.2"E
81	DUZCE	17,072	149	40°50′37.2"N—31°08′55.5"E

Automatic Meteorological Observation Stations (OMGI). The missing data, which were very small in number, were completed from the Manual Observation Stations of the same stations. The central stations of 37 provinces that can represent Turkey were identified and statistically analyzed. These 37 stations, whose details are given in Table 1, cover the entire geographical area of Turkey, taking into account the sensitivity of precipitation and temperature data. In addition, in order to obtain more precise and accurate results in the study, the height and distance of the stations from sea level were taken into account both in drought analysis and in the mapping process in GIS systems. In this study, the main use of stochastic time series models is that they are one of the methods that have been used for a long time and give good results. These models are particularly good for predicting the future behavior of time series under certain conditions. In addition, these models work under the assumption of linear and stationary time series and often provide more interpretable and understandable results. Especially with complex and long-term data such as meteorological data, it is important to understand how the model works. (Al-Najjar et al., 2020; Papacharalampous et al., 2019).

Precipitation in Turkey varies between 250 and 2500 mm/year according to regions. It is the least rainfall region of Turkey with 1000–2500 mm/year in coastal regions, 500–1000 mm/year in inland regions and 250–300 mm/year around Tuz Lake in Central Anatolia.

2.3. Autocorrelation Function (ACF)

The autocorrelation function (ACF) is a statistical method that measures the linear connection between data by analyzing lags in time series. It also identifies the strength and presence of autocorrelation. It provides information about the correlation between some values of a data set and its lagged values (Box et al., 2008; Kashyap & Rao, 1976). The autocorrelation between X_t and X_{t+k} values in a data set is given in Eq. 1.

$$\rho_k = \frac{cov(x_t, x_{t+k})}{\sigma_t . \sigma_{t+k}} \tag{1}$$

In Eq. 1: ρ_k: Autocorrelation value between data, x_t: Original data in time series, x_{t+k}: Data with a lag of k in the time series, $cov(x_t, x_{t+k})$: Auto covariance between data, σ_t: Variance of the original data series without lag, σ_t: denotes the variance of the data series with k lags. ACF is obtained by calculating the correlation coefficient between the lagged value of the data in a data set. ACF graph is then obtained by placing lag values on the x-axis and correlation coefficient values on the y-axis on the cartesian system. Correlation coefficient values are between −1 and 1. Negative values indicate negative autocorrelation (data that are contrary to each other over time), positive values indicate positive autocorrelation (data that are similar to each other over time), and 0 indicates no autocorrelation.

ACF graphs serve several different purposes. First, ACF plots help to detect trends and patterns in a data set. If there is a rapid decline in ACF values, it indicates that there is no autocorrelation or weak autocorrelation in the data set. On the other hand, if there is a slow decline in ACF values, it indicates that there is an interaction between past values and future values and a strong autocorrelation in the data set. Another use of ACF plots is to help determine the appropriate lag order of the data set for autoregressive (AR) or moving average (MA) models. Using these plots, the number of lagged observations used to estimate the current observation is obtained. Finally, the stationarity of a data set can be understood from ACF plots. For stationary series, the ACF value declines rapidly and does not stay within the confidence interval. If ACF values exhibit a slow decline or large peaks outside the confidence interval, this indicates instability and may require further analysis or differentiation to stabilize the series. In brief, ACF provides information about the structure of the data within a time series. It also helps to identify this structure, assess the stationarity of the series and determine the lag order. By analyzing ACF plots, more accurate forecasts and models can be obtained for time series data.

2.4. Partial Autocorrelation Function (PACF)

The partial autocorrelation function (PACF) is a statistical model used to measure the linear relationship between time series observations at different lags. PACF provides information about the degree of dependence between the data set and the lagged data set and controls for the effect of intermediate lags. Similar to ACF graphs, PACF graphs are obtained by placing lags on the x-axis and PACF values on the Y-axis on the caartesian system. PACF values range from −1 to 1, where 0 indicates no correlation, 0–1 indicates positive partial autocorrelation and −1 to 0 indicates negative partial autocorrelation. ACF and PACF are statistical models used to analyze correlations between observations in a time series. However, there are important differences between them: ACF measures the correlation between an observation and its lagged values, while PACF controls for the effect of intermediate lags and measures the correlation between an observation and its lagged values. ACF measures direct and indirect relationships and the overall relationship between observations in lags. PACF, on the other hand, focuses only on the direct relationship between an observation and its specific lag, without including the effect of intermediate lags. ACF plot is used to rank MA expressions in an ARIMA model. The damping of ACF plot helps to identify important MA terms. On the other hand, PACF plot is used to determine the order of AR terms

in ARIMA model. Significant partial autocorrelation values in PACF plot indicate significant AR terms.

2.5. Auto Regressive Integrated Moving Average (ARIMA) Models

ARIMA is a statistical time series model. This model analyzes time series data and provides forward-looking forecasting of this data set. ARIMA models can be used in many different fields such as engineering, economics, meteorology and energy. ARIMA model consists of three main components. These components are autoregressive component (AR), (I) derivative component and MA component. AR component takes into account the relationship between a parameter in the data set and the previous parameter and the future data can be predicted from the past data, while MA component takes into account the relationship between the errors of the data and the past forecast. The derivative component is used to eliminate the trend in the data set. ARIMA models are also represented by (p, d, q). ARIMA models are a type of Box Jekins Stochastic time series models and their mathematical expression is given in Eq. 2 (Box & Jenkins, 1976).

$$z_t = \phi_1 z_{t-1} + \phi_2 z_{t-2} + \ldots + \phi_p z_{t-p} + \delta + \epsilon_t - \theta_1 \epsilon_{t-1} + \theta_2 \epsilon_{t-2} + \ldots + \theta_p \epsilon_{t-q} \quad (2)$$

In Eq. 2; Z_t, Z_{t-1},…, Z_{t-p} d order-differenced observation values, $\phi_1, \phi_2 \ldots \phi_p$ coefficients for observation values differenced by d orders, δ constant value, $\epsilon_t, \epsilon_{t-1}, \epsilon_{t-2} \ldots \epsilon_{t-q}$ error terms ve $\theta_1, \theta_2 \ldots \theta_p$ coefficients related to error terms.

2.6. Seasonal Auto Regressive Integrated Moving Average (SARIMA) Models

In some cases, ARIMA models are inadequate to analyze data sets that have the effect of seasonality in them. ARIMA models are extended and SARIMA models are obtained. In particular, SARIMA models are used to analyze data with recurring seasonality effects. In addition to ARIMA models, SARIMA models are analyzed once again with ACF and PACF by taking the seasonal difference of the data. SARIMA is represented by the expression (p,d,q)(P, D, Q)s.

2.7. Standard Precipitation-Evapotranspiration Index (SPEI)

It is known that the complex structure of drought analyses has been addressed and different indices (indicators) have been designed for this situation. Indices calculated for drought analyses; SPI, palmer drought severity index (PDSI), reconnaissance drought index (RDI), SPE), joint drought index (JDI), triple drought index (TDI), multivariate standardized drought index (MSDI), multivariate drought index (MDI) can be given as examples. SPEI will be used in this study. SPEI is one of the most widely used drought indices for monitoring and assessing drought conditions. SPEI analyzes drought by integrating both precipitation, evaporation and potential transpiration (evapotranspiration) (PET) data. Thus, the main feature that distinguishes SPEI indicator from other indicators is that it takes into account not only the lack of precipitation but also the evaporation demand of the atmosphere (PET). By taking both factors into account, SPEI provides a more comprehensive understanding of drought conditions than other indices based on rainfall alone.

SPEI has proven to be an index that can be used in various fields, including agriculture, water resources management and climate studies. By providing information on the severity, duration and frequency of drought events, it helps decision-making processes related to drought mitigation, water allocation and land management. SPEI derives its drought analyses by standardizing PET and precipitation data. This standardized data allows the comparison of drought severity, frequency and duration for different regions and time periods. SPEI was introduced by Vicente-Serrano et al. (2010).

The basic mathematical expression of SPEI is given in Eq. 3.

$$SPEI = W - \frac{2.516 + 0.803W + 0.01W^2}{1 + 1.433W + 0.189W^2 + 0.001W^3} \quad (3)$$

where;

$$W = \sqrt{-2\ln(P)} P \leq 0.5 \quad (4)$$

P is the probability of exceeding any D_i value and is given in Eq. 5.

$$P = 1 - f(x) \tag{5}$$

The expression of D_i is given in Eq. 6.

$$D_n^k = \sum_{i-0}^{k-1} P_{n-1} - (PET)_{n-1} \tag{6}$$

Log-logistic distribution of SPEI density function is given in Eq. 6. In addition, Potential Evapotranspiration PET will be analyzed by Thornthwaite equation. The mathematical expression of PET for the Thornthwaite equation is given in Eq. 7 (Thornthwaite, 1948).

$$f(x) = \frac{\beta}{\alpha} \cdot \left(\frac{x-y}{\alpha}\right)^{\beta-1} \left(1 + \left(\frac{x-y}{\alpha}\right)^{\beta}\right)^{-2} \tag{7}$$

$$PET = 16 \times \left(\frac{N}{12}\right) \times \left(\frac{m}{30}\right) \times \left(10 \times \frac{T_{average}}{I}\right)^{\alpha} \tag{8}$$

N: Average day length of the calculated month (hours), m: Number of days in the calculated month, $T_{average}$: Daily average temperature value, I: Heat index based on 12-month average temperatures, α: The coefficient depending on the calculated temperature index. By looking at SPEI results, the degree of drought or humidity in the region can be determined. If SPEI values are positive, it is concluded that there is humidity in the region, and if SPEI values are negative, it is concluded that there is drought in the region. The drought classification of SPEI is given in Table 2.

Table 2

SPEI Drought Classifications

SPEI Values	Drought Classification
-2.00 and below	Extremely Dry
− 1.50 to − 1.99	Severely Dry
− 1.00 to − 1.49	Moderate dry
− 0.99 to 0	Mild dry
0 to 0.99	Mild Wet
1 to 1.49	Moderate Wet
1.50 to 1.99	Severely Wet
2 and above	Extremely Wet

3. Result and Discussion

3.1. Analysis and Modeling of Stochastic Time Series

R_Statistical analysis language and statistical software package, which are recommended to be used in research and academic studies, were used in order to analyze the daily total precipitation and daily average temperature data provided by Mgm in a safe and high quality manner. It is seen that both software languages are frequently used in time series data and especially in the analysis of climate and meteorological data and successful results are obtained. Therefore, in this part of the study, these two software packages were used to analyze and model the data. Time series data were analyzed by ACF, PACF and Correlogram analyses. In addition, stationarity tests of both precipitation and temperature time series data were applied with augmented dickey-fuller (ADF). If ADF test yields a p-value less than 5%, the null hypothesis is rejected and the time series is stationary (Al-Najjar et. al., 2020). On the contrary, it means that the data set contains a trend and this data set should be stationary by taking the difference. Figure 4 shows an example of the ACF, stationarized ACF, PACF and stationarized PACF plots for the temperature data of Mersin province.

When Fig. 4 is examined, it is seen that the relationship between the data in the behavioral process of the temperature data of Mersin province is seasonally high and in order to remove this excessive relationship, the data set was stationary by taking the difference. In addition, in the correlogram analysis, it was concluded that the time series repeats every 12 months, so seasonal analysis should be 12 months. In addition, as a result of the interpretation of the graphs in Fig. 4, it was concluded that SARIMA model of Mersin province temperature data is $(2,0,2)(5,1,1)_{12}$. In addition, ACF and PACF analyses of the temperature data of 37 stations were performed and model results were obtained. As a result of ACF and PACF analysis of the temperature data of 37 stations, a SARIMA model suitable for each station was created. In the correlogram analysis, the seasonality effect was taken as 12 months in all stations since the frequency was 12 months in all stations. The temperature time series

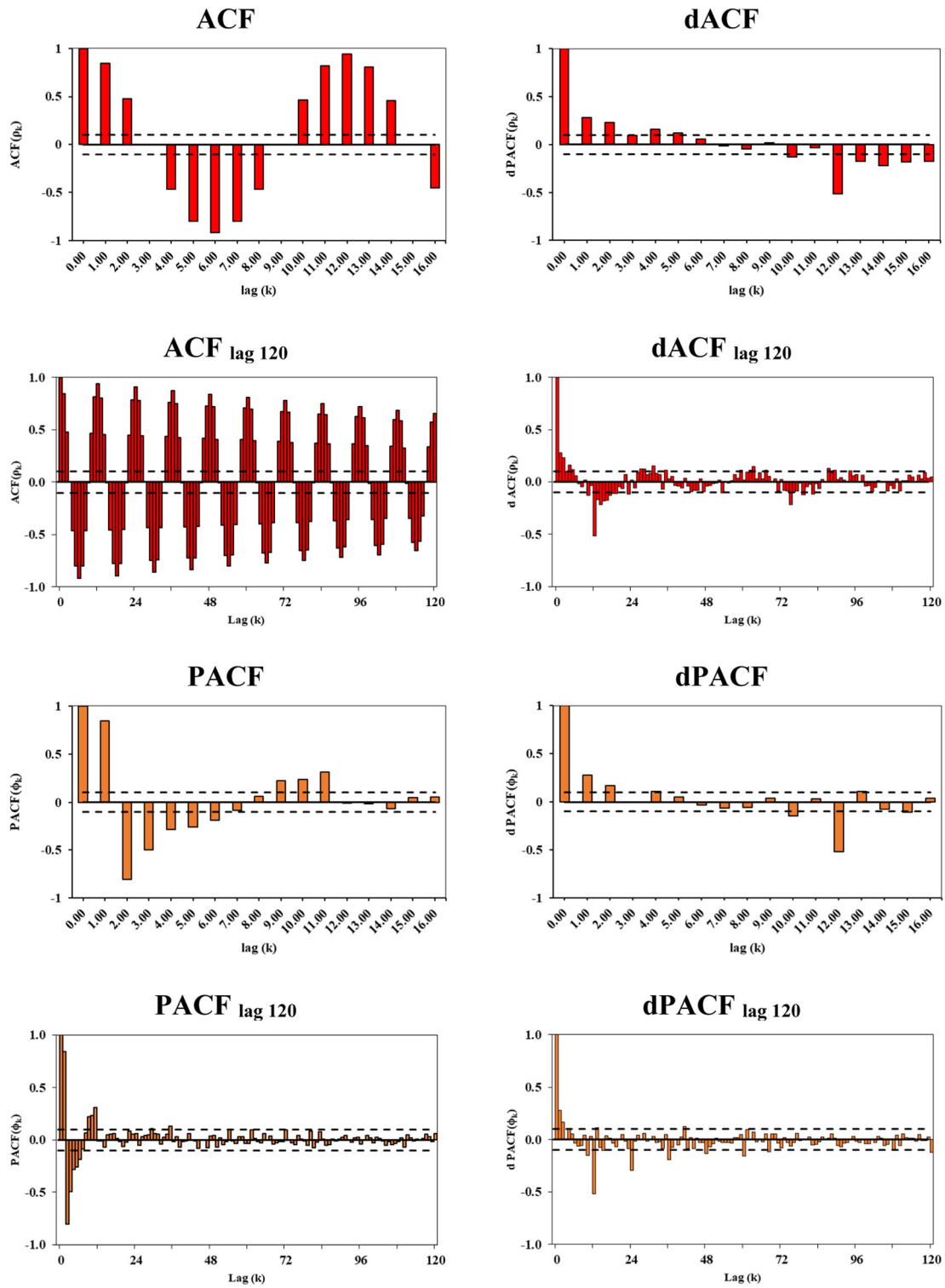

Figure 4
Analysis of Mersin Province Temperature Data

Table 3

Temperature SARIMA Model of 37 Stations

Station	ARIMA	SARIMA	Station	ARIMA	SARIMA
AFYON	(2.0.2)	(3.1.1)	KONYA	(2.0.4)	(6.1.2)
ANKARA	(5.2.3)	(2.1.3)	KUTAHYA	(2.0.2)	(3.1.1)
ANTALYA	(6.2.4)	(3.1.5)	MALATYA	(1.0.4)	(3.1.1)
AYDIN	(6.2.4)	(6.1.7)	MUGLA	(2.0.2)	(5.1.1)
BALIKESIR	(1.0.4)	(3.1.1)	MUS	(1.0.3)	(3.1.1)
BILECIK	(1.0.2)	(5.1.1)	NIGDE	(1.0.2)	(3.1.1)
CANAKKALE	(1.0.2)	(5.1.1)	SAMSUN	(1.0.1)	(5.1.1)
CANKIRI	(3.0.1)	(5.1.3)	SIVAS	(1.0.4)	(5.1.2)
DIYARBAKIR	(7.2.2)	(4.1.4)	TRABZON	(1.0.8)	(5.1.1)
EDIRNE	(1.0.2)	(3.1.1)	TUNCELI	(2.0.4)	(5.1.1)
ERZINCAN	(1.0.2)	(3.1.1)	SANLIURFA	(2.0.5)	(5.1.1)
ERZURUM	(4.1.2)	(3.1.4)	VAN	(1.0.3)	(3.1.1)
GAZIANTEP	(4.1.1)	(3.1.2)	YOZGAT	(1.0.1)	(3.1.1)
MERSIN	(2.0.2)	(5.1.1)	SIRNAK	(1.0.3)	(3.1.1)
ISTANBUL	(6.1.1)	(3.1.2)	ARDAHAN	(1.0.4)	(4.1.1)
IZMIR	(2.0.2)	(5.1.3)	IGDIR	(1.0.4)	(4.1.1)
KASTAMONU	(1.0.1)	(3.1.1)	OSMANIYE	(3.0.5)	(4.1.1)
KAYSERI	(1.0.2)	(3.1.1)	DUZCE	(1.0.4)	(3.1.1)
KIRSEHIR	(1.0.4)	(6.1.1)			

SARIMA model for the 37 stations analyzed are given in Table 3.

In addition, daily total precipitation data of 37 stations were analyzed in this part of the study. As a result of ACF and PACF analysis graphs of the precipitation data of 37 stations, a SARIMA model suitable for each station was created. Since the frequency in the correlogram analysis of all stations is 12 months, the seasonality effect is taken as 12 months in all stations. SARIMA model of precipitation time series for the 37 stations analyzed is given in Table 4.

3.2. Model Estimation and Validation

Stochastic model structures of time series data were obtained with R_Statistical analysis software. As an example of the parameters obtained as a result of the analysis, the parameters of Afyon province are given in Table 5.

The process given as an example in Table 5 was carried out for all selected cities. With the SARIMA models built, 90% of the temperature and precipitation data between 1990 and 2020 were used for training while 10% were used for testing. Daily average temperature and daily total precipitation time series data were predicted until 2050 with SARIMA models. The 2050 daily average temperature and daily total precipitation data were verified by correlation analysis r and root mean square error (RMSE) analysis. A summary of the prediction and analysis results of the SARIMA model is given in Table 6.

As a result, when Table 6 is analyzed, according to SARIMA model, the average r value is 99% and RMSE value is 1.46 for temperature time series data. In the precipitation time series data, the average r value was calculated as 66% and RMSE value as 34.6. SPEI drought analysis of Turkey was obtained by using precipitation and temperature data predicted until 2050 with the help of Stochastic Time Series models. SPEI3, SPEI6, SPEI9 and SPEI12 drought analyses for 4 different time periods were performed. Potential Evapotranspiration (PET) was calculated with the Thornthwaite model in the stud. Climate water balance (CWBAL) was calculated based on PET values obtained. With the completion of these processes, SPEI values were calculated. Drought return period maps of Turkey were created by analyzing SPEI values obtained in the study. These maps were prepared for 4 different time scales

(SPEI3, SPEI6, SPEI9 and SPEI12). The drought return period map of Turkey, which expresses how often drought occurs at each time scale, is given in Fig. 5.

When the $SPEI_3$ drought return period map is examined in Fig. 5, it is seen that droughts are experienced in 0–10 and 10–20 periods across Turkey. However, it is concluded that droughts may occur in 20–30 periods of 3 months in Mugla, Antalya, Mersin, Adana, Sanliurfa, Sirnak, Tunceli, Erzurum, Kastamonu, Cankiri and Kutahya. When the $SPEI_6$ drought return period map is examined, it is seen that droughts are experienced in 0–10 and 10–20 periods across Turkey. However, it is concluded that droughts may occur in Mugla, Antalya, Mersin, Adana, Sirnak, Van, Tunceli, Erzurum, Kastamonu, Cankiri, Ankara and Kutahya in a 6-month period of 20–30 periods. When the $SPEI_9$ drought return period map is examined, it is seen that droughts are experienced in 0–10 and 10–20 periods across Turkey. However, it is concluded that droughts may occur in Mugla, Antalya, Mersin, Sanliurfa, Sirnak, Tunceli, Kastamonu, Ankara and Kutahya for 20–30 periods and in Cankiri for 30–40 periods in 9-month period. When the $SPEI_{12}$ drought return period map is examined, it is seen that droughts are experienced in 0–10 and 10–20 periods across Turkey. However, it is concluded that Antalya, Mersin, Sirnak, Tunceli, Ankara and Kutahya provinces may experience drought in 20–30 periods, and Mugla, Kastamonu and Cankiri provinces may experience drought in 30–40 periods in 12-month period. In addition, drought maps of Turkey for 4 different time scales ($SPEI_3$, $SPEI_6$, $SPEI_9$ and $SPEI_{12}$) were created to cover the period between 1990 and 1999, 2000–2009, 2010–2019, 2020–2029, 2030–2039 and 2040–2049. Figure 6 shows the drought maps of $SPEI_3$ and $SPEI_6$ for the period 1990–2050.

When Fig. 6 is examined, in the $SPEI_3$ drought map of Turkey between 1990 and 2050; it is seen that the drought indicator SPEI value is between 0 and 0.5 in Turkey between 1990 and 1999. However, in Istanbul, Antalya, Konya, Ankara, Diyarbakır, Mus, Erzincan, Sivas, Kirsehir and Nigde, the drought indicator is between 0.5 and 1. In Ardahan, Balıkesir, Mugla, Osmaniye, Sirnak, Hakkari, Siirt and Kastamonu provinces, the SPEI drought indicator is between 0 and −0.5. Between 2000 and 2009, the drought indicator SPEI value was between 0 and 0.5 and 0−−0.5 in Turkey. However, in Istanbul, Antalya

Table 4

Precipitation SARIMA Model for 37 Stations

Station	ARIMA	SARIMA	Station	ARIMA	SARIMA
AFYON	(0.0.0)	(5.1.1)	KONYA	(8.0.1)	(7.1.2)
ANKARA	(1.2.11)	(2.1.3)	KUTAHYA	(2.0.2)	(6.1.1)
ANTALYA	(11.2.1)	(6.1.1)	MALATYA	(2.0.2)	(4.1.1)
AYDIN	(11.2.2)	(4.1.1)	MUGLA	(0.0.0)	(6.1.1)
BALIKESIR	(1.0.1)	(3.1.1)	MUS	(8.0.1)	(7.1.1)
BILECIK	(7.0.2)	(4.1.2)	NIGDE	(1.0.1)	(5.1.2)
CANAKKALE	(0.0.0)	(7.1.1)	SAMSUN	(1.0.1)	(6.1.1)
CANKIRI	(8.0.1)	(7.1.1)	SIVAS	(1.0.1)	(5.1.1)
DIYARBAKIR	(7.0.5)	(3.1.2)	TRABZON	(1.0.1)	(6.1.1)
EDIRNE	(11.0.2)	(5.1.2)	TUNCELI	(0.0.0)	(5.1.1)
ERZINCAN	(7.0.2)	(6.1.1)	SANLIURFA	(0.0.0)	(6.1.1)
ERZURUM	(3.1.1)	(4.1.1)	VAN	(0.0.0)	(5.1.1)
GAZIANTEP	(5.1.1)	(3.1.2)	YOZGAT	(7.0.2)	(6.1.1)
MERSIN	(0.0.0)	(6.1.1)	SIRNAK	(7.0.1)	(6.1.1)
ISTANBUL	(12.2.2)	(4.1.2)	ARDAHAN	(0.0.0)	(5.1.1)
IZMIR	(1.0.1)	(3.1.1)	IGDIR	(1.0.1)	(3.1.1)
KASTAMONU	(2.0.2)	(4.1.1)	OSMANIYE	(8.0.1)	(6.1.1)
KAYSERI	(7.0.1)	(6.1.1)	DUZCE	(0.0.0)	(6.1.2)
KIRSEHIR	(0.0.0)	(6.1.1)			

Table 5

SARIMA Model Parameters for Afyon Province

Station	Non-Seasonal Parameters				Seasonal Parameters					
	Φ_1	Φ_2	Θ_1	Θ_2	Φ_1	Φ_2	Φ_3	Φ_4	Φ_5	Θ_1
Afyon (temperature)	−0.26	0.17	0.58	0.03	−0.08	−0.01	−0.09	–	–	−0.69
Afyon (precipitation)	–	–	–	–	−0.02	0.006	0.09	−0.03	−0.03	−1.00

Table 6

SARIMA Model Prediction and Analysis Results Overview

City	Temperature				Precipitation			
	ARIMA	SARIMA	r	RMSE (°C)	ARIMA	SARIMA	r	RMSE (mm)
AFYON	(2.0.2)	(3.1.1)	96%	2.1	(0.0.0)	(5.1.1)	41%	25.9
ANKARA	(5.2.3)	(2.1.3)	98%	1.3	(1.2.11)	(2.1.3)	60%	21.3
ANTALYA	(6.2.4)	(3.1.5)	99%	1	(11.2.1)	(6.1.1)	70%	82.9
AYDIN	(6.2.4)	(6.1.7)	99%	1.1	(11.2.2)	(4.1.1)	82%	27.8
BALIKESIR	(1.0.4)	(3.1.1)	98%	1.4	(1.0.1)	(3.1.1)	62%	28.2
BILECIK	(1.0.2)	(5.1.1)	98%	1.4	(7.0.2)	(4.1.2)	72%	25.4
CANAKKALE	(1.0.2)	(5.1.1)	98%	1.3	(0.0.0)	(7.1.1)	59%	33.2
CANKIRI	(3.0.1)	(5.1.3)	99%	1.6	(8.0.1)	(7.1.1)	76%	20.7
DIYARBAKIR	(7.2.2)	(4.1.4)	99%	1.4	(7.0.5)	(3.1.2)	70%	28.7
EDIRNE	(1.0.2)	(3.1.1)	99%	1.4	(11.0.2)	(5.1.2)	58%	36.9
ERZINCAN	(1.0.2)	(3.1.1)	99%	1.6	(7.0.2)	(6.1.1)	61%	17.5
ERZURUM	(4.1.2)	(3.1.4)	99%	1.5	(3.1.1)	(4.1.1)	68%	22.7
GAZIANTEP	(4.1.1)	(3.1.2)	99%	1.2	(5.1.1)	(3.1.2)	75%	42
MERSIN	(2.0.2)	(5.1.1)	99%	1	(0.0.0)	(6.1.1)	79%	74.4
ISTANBUL	(6.1.1)	(3.1.2)	98%	1.3	(12.2.2)	(4.1.2)	55%	51.6
IZMIR	(2.0.2)	(5.1.3)	99%	1.3	(1.0.1)	(3.1.1)	67%	58.8
KASTAMONU	(1.0.1)	(3.1.1)	99%	1.4	(2.0.2)	(4.1.1)	73%	28.9
KAYSERI	(1.0.2)	(3.1.1)	99%	1.6	(7.0.1)	(6.1.1)	60%	18.7
KIRSEHIR	(1.0.4)	(6.1.1)	99%	1.6	(0.0.0)	(6.1.1)	53%	21.1
KONYA	(2.0.4)	(6.1.2)	99%	1.4	(8.0.1)	(7.1.2)	65%	22.1
KUTAHYA	(2.0.2)	(3.1.1)	98%	1.5	(2.0.2)	(6.1.1)	69%	23
MALATYA	(1.0.4)	(3.1.1)	99%	1.7	(2.0.2)	(4.1.1)	63%	23.9
MUGLA	(2.0.2)	(5.1.1)	99%	1.2	(0.0.0)	(6.1.1)	75%	73.8
MUS	(1.0.3)	(3.1.1)	98%	2	(8.0.1)	(7.1.1)	72%	39.7
NIGDE	(1.0.24	(3.1.1)	98%	1.5	(1.0.1)	(5.1.2)	65%	20
SAMSUN	(1.0.1)	(5.1.1)	98%	1.2	(1.0.1)	(6.1.1)	69%	27.2
SIVAS	(1.0.4)	(5.1.2)	98%	1.7	(1.0.1)	(5.1.1)	60%	23.5
TRABZON	(1.0.8)	(5.1.1)	98%	1.2	(1.0.1)	(6.1.1)	56%	38.9
TUNCELI	(2.0.4)	(5.1.1)	99%	1.5	(0.0.0)	(5.1.1)	74%	46.2
SANLIURFA	(2.0.5)	(5.1.1)	99%	1.4	(0.0.0)	(6.1.1)	65%	32
VAN	(1.0.3)	(3.1.1)	99%	1.2	(0.0.0)	(5.1.1)	61%	21.3
YOZGAT	(1.0.1)	(3.1.1)	98%	1.7	(7.0.2)	(6.1.1)	79%	24.8
SIRNAK	(1.0.3)	(3.1.1)	99%	1.2	(7.0.1)	(6.1.1)	71%	59.3
ARDAHAN	(1.0.4)	(4.1.1)	98%	1.7	(0.0.0)	(5.1.1)	72%	24.8
IGDIR	(1.0.4)	(4.1.1)	98%	2.8	(1.0.1)	(3.1.1)	70%	13.8
OSMANIYE	(3.0.5)	(4.1.1)	99%	1.2	(8.0.1)	(6.1.1)	60%	48.5
DUZCE	(1.0.4)	(3.1.1)	98%	1.5	(0.0.0)	(6.1.2)	55%	30.6

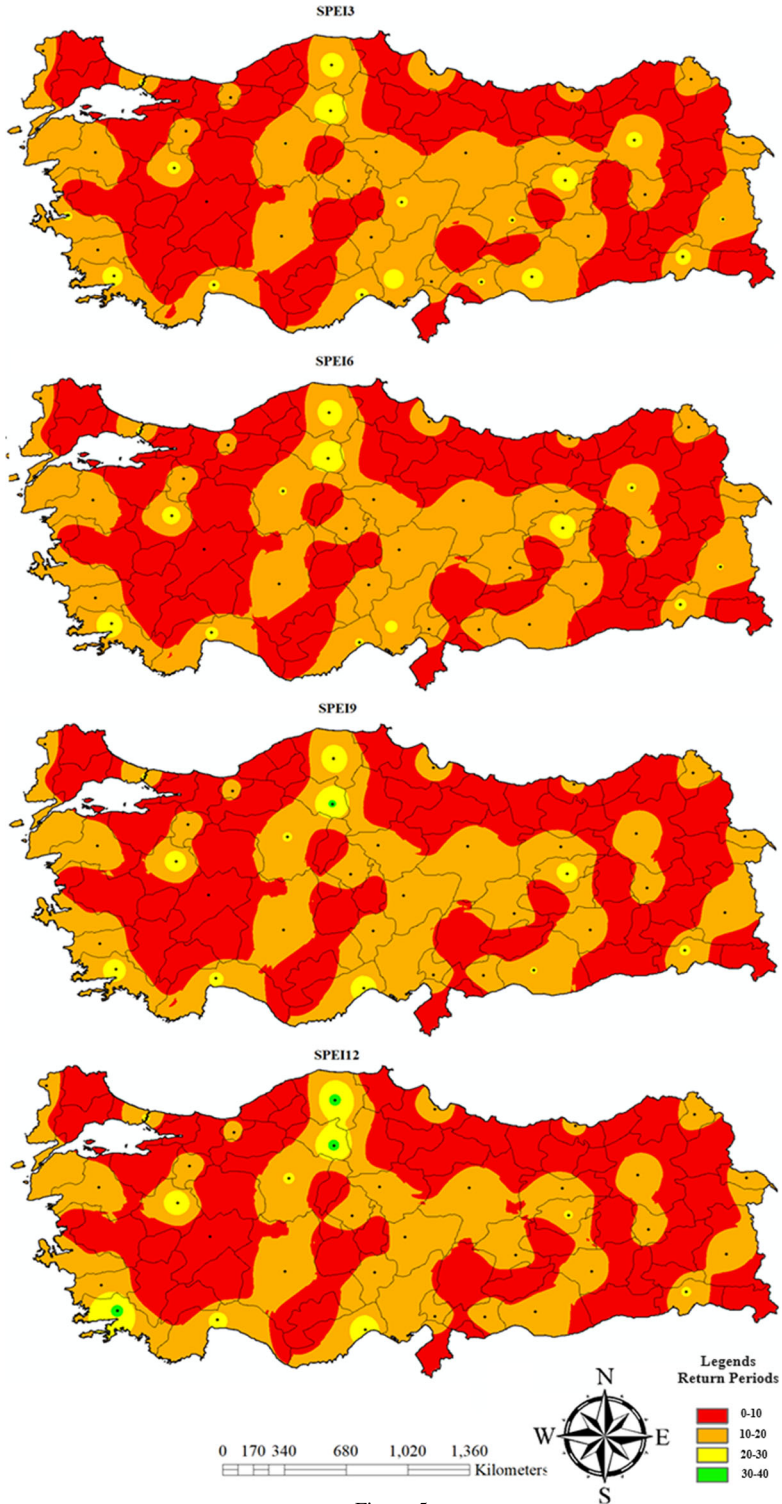

Figure 5
Drought Return Period Map of Turkey

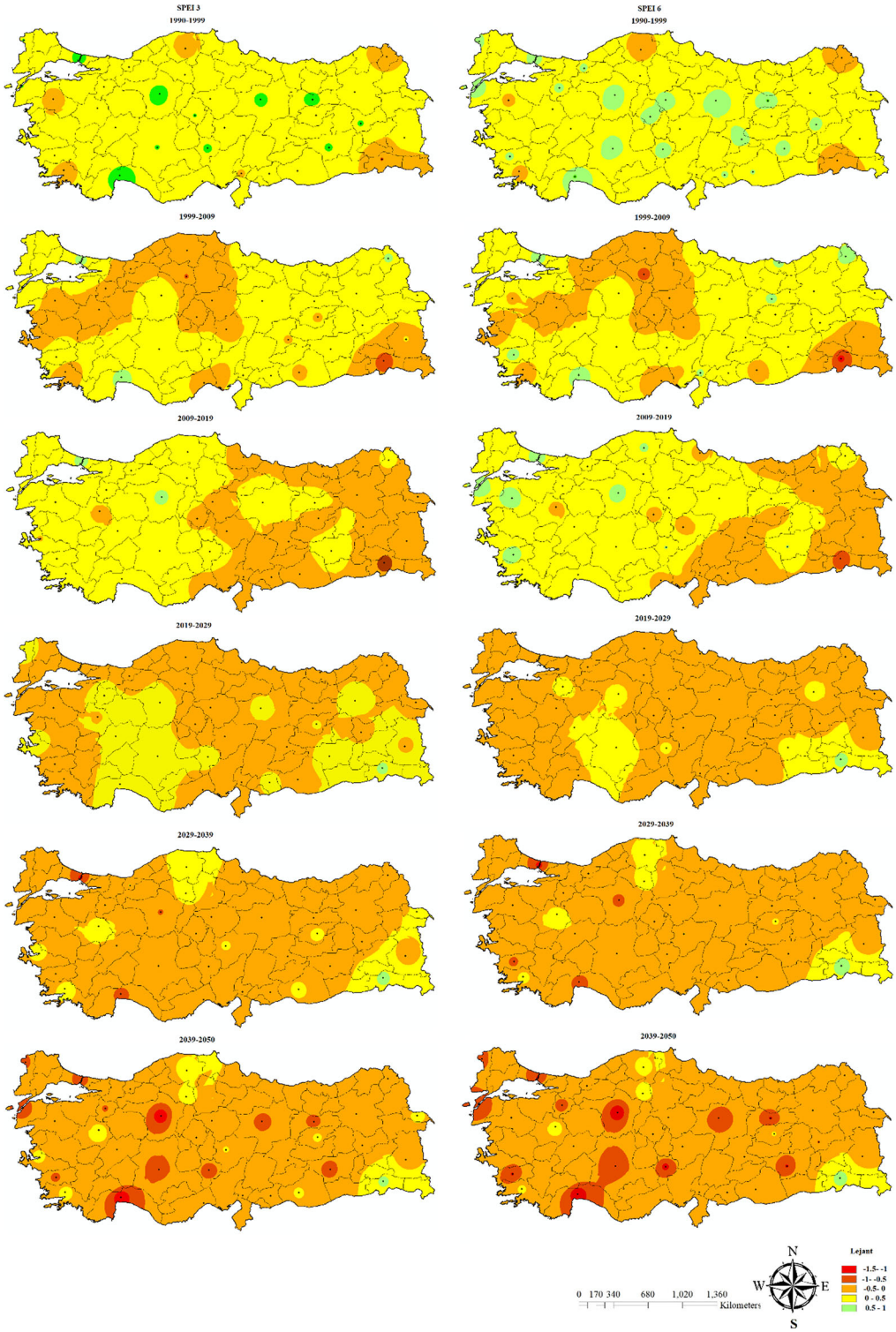

Figure 6
Turkey 1990–2050 $SPEI_3$ and $SPEI_6$ Drought Map

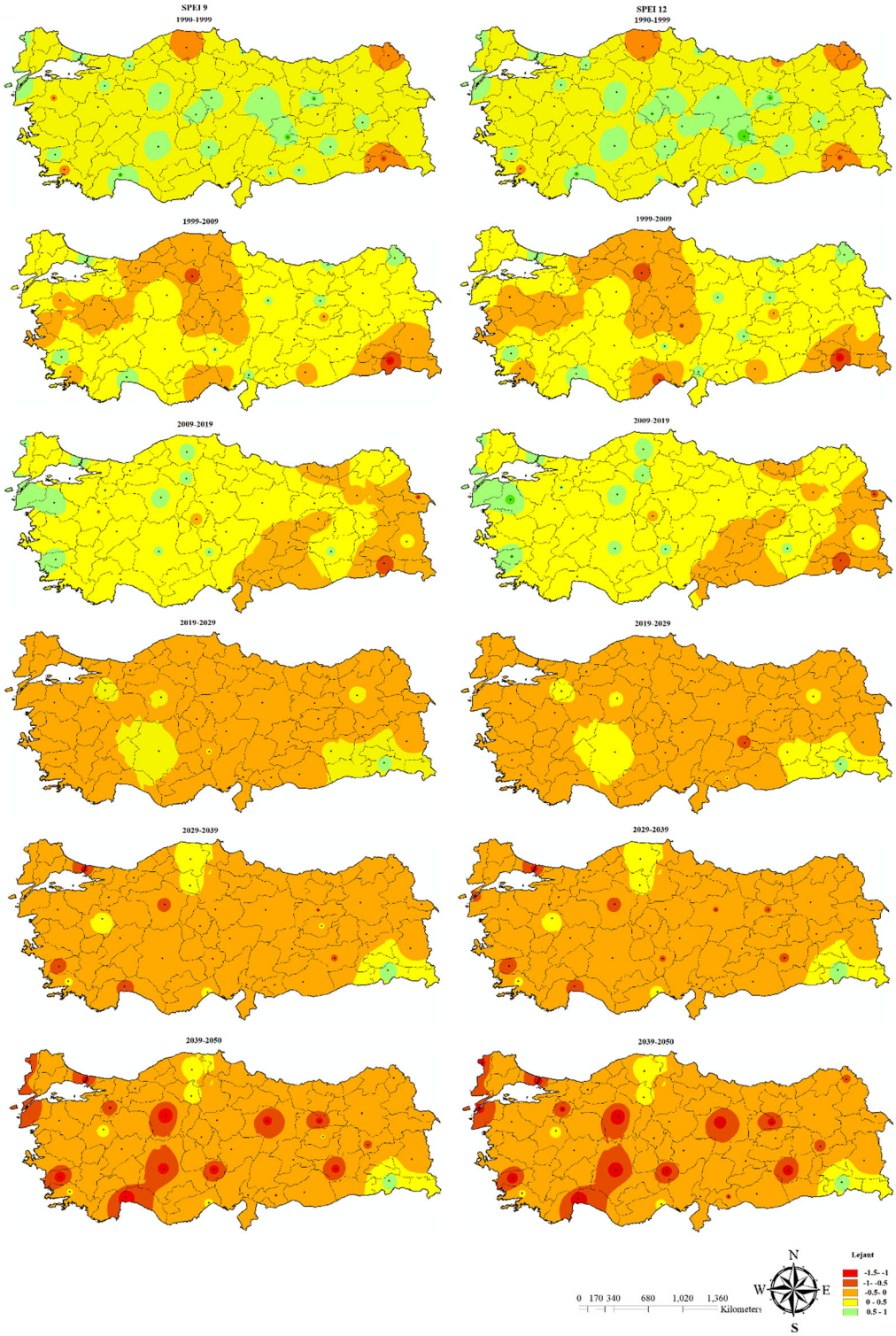

Figure 7
Turkey 1990–2050 $SPEI_9$ and $SPEI_{12}$ Drought Map

and Ardahan provinces, the drought indicator is between 0.5 and 1. In Sirnak province, the drought indicator was calculated to be between -0.5–−1. Between 2010 and 2019, the drought indicator SPEI value was between 0 and 0.5 and 0–−0.5 in Turkey. However, in Istanbul and Ankara, the drought indicator is between 0.5 and 1. In Sirnak province, the drought indicator was calculated between −0.5−1. 2020–2029 drought indicator SPEI value is between 0 and 0.5 and 0–−0.5 values in Turkey. However, in Sirnak province, the drought indicator was calculated to be between 0.5 and 1 values. In 2030–2039, the drought indicator SPEI value is between 0 and −0.5 values in Turkey. However, the drought indicator values of Istanbul, Ankara and Antalya provinces are between −0.5–−1 values and the drought indicator in Sirnak province is between 0.5 and 1 values. Between the years 2040–2049, the drought indicator SPEI value is between 0 and −0.5 values in Turkey. However, drought indicator values of Istanbul, Edirne, Canakkale, Bilecik, Aydin, Konya, Nigde, Diyarbakır, Erzincan, Erzincan, Sivas, Ankara and Antalya provinces are between −1.5–−1 values and drought indicator in Sirnak province is between 0.5 and 1 values.

In the $SPEI_6$ drought map of Turkey between 1990 and 2050; it was observed that the drought indicator SPEI value was between 0 and 0.5 in Turkey between 1990 and 1999. However, in Istanbul, Edirne, Canakkale, Aydin, Antalya, Konya, Nigde, Gaziantep, Ankara, Bilecik, Karabuk, Diyarbakır, Mus, Erzincan, Sivas, Malatya, Kirsehir and Yozgat, the drought indicator is between 0.5 and 1. In Ardahan, Balıkesir, Mugla, Sirnak, Siirt and Kastamonu provinces, SPEI drought indicator is between 0 and −0.5. Between 2000 and 2009, the drought indicator SPEI value was between 0 and 0.5 and 0–−0.5 in Turkey. However, in the provinces of Istanbul, Aydin, Antalya, Erzincan, Trabzon and Ardahan, the drought indicator is between 0.5 and 1. In Sirnak and Cankiri provinces, the drought indicator was calculated to be between −0.5–−1. Between 2010 and 2019, the drought indicator SPEI value was between 0 and 0.5 and 0–−0.5 in Turkey. However, in Istanbul, Canakkale, Balıkesir, Aydin, Kastamonu and Ankara, the drought indicator is between 0.5 and 1. In Sirnak province, the drought indicator was calculated to be between −0.5–−1. Between the years 2020–2029, the drought indicator SPEI value was found to be between 0 and −0.5 values in Turkey. However, in Sirnak province, the drought indicator was calculated to be between 0.5 and 1. Between the years 2030–2039, the drought indicator SPEI value is between 0 and −0.5 values in Turkey. However, the drought indicator values of Istanbul, Aydin, Ankara and Antalya provinces are between −0.5–−1 values and the drought indicator in Sirnak province is between 0.5 and 1 values. Between the years 2040–2049, the drought indicator SPEI value is between 0 and −0.5 values in Turkey. However, the drought indicator values of Istanbul, Edirne, Canakkale, Bilecik, Aydin, Konya, Nigde, Diyarbakır, Erzincan, Sivas, Ankara and Antalya provinces are between −1.5–−1 values and the drought indicator in Sirnak province is between 0.5 and 1 values. In addition, Fig. 7 shows the drought maps of $SPEI_9$ and $SPEI_{12}$ for the period 1990–2050.

When Fig. 7 is examined, in the $SPEI_9$ drought map of Turkey between 1990 and 2050, it is seen that the drought indicator SPEI value is between 0 and 0.5 in Turkey between 1990and 1999. However, in Istanbul, Edirne, Canakkale, Aydin, Antalya, Konya, Nigde, Ankara, Bilecik, Karabuk, Gaziantep, Sanliurfa, Diyarbakır, Mus, Erzincan, Sivas, Malatya, Kirsehir and Yozgat, the drought indicator is between 0.5 and 1. In Ardahan, Balıkesir, Mugla, Sirnak, Siirt and Kastamonu provinces, the SPEI drought indicator is between 0 and −0.5. Between the years 2000–2009, the drought indicator SPEI value was between 0 and 0.5 and 0–−0.5 in Turkey. However, in Istanbul, Aydin, Antalya, Osmaniye, Nigde, Erzincan, Sivas, Trabzon and Ardahan, the drought indicator is between 0.5 and1. In Sirnak and Cankiri provinces, the drought indicator was calculated to be between −0.5–−1. Between 2010–2019, the drought indicator SPEI value was between 0 and 0.5 and 0–−0.5 in Turkey. However, in Istanbul, Edirne, Canakkale, Balıkesir, Aydin, Konya, Nigde, Cankiri, Diyarbakır, Kastamonu and Ankara, the drought indicator is between 0.5 and 1. In Sirnak and Iğdır provinces, the drought indicator was calculated to be between -0.5 and -1. It was observed that the drought indicator SPEI value was between 0 and −0.5 values in Turkey between 2020 and 2029. However, it is

calculated that the drought indicator in Sirnak province is between 0.5 and 1 values. Between the years 2030–2039, the drought indicator SPEI value is between 0 and −0.5 values in Turkey. However, the drought indicator values of Istanbul, Ankara, Aydin, Diyarbakır, Erzincan and Antalya provinces are between −0.5–−1 values and the drought indicator in Sirnak province is between 0.5 and 1 values. Between the years 2040–2049, the drought indicator SPEI value is between 0 and −0.5 values in Turkey. However, drought indicator values of Istanbul, Edirne, Canakkale, Bilecik, Aydin, Konya, Nigde, Diyarbakır, Mus, Erzincan, Sivas, Ankara and Antalya provinces are between −1.5–−1 values and drought indicator in Sirnak province is between 0.5 and 1 values.

In the $SPEI_{12}$ drought map of Turkey between 1990 and 2050; it was observed that the drought indicator SPEI value was between 0 and 0.5 in Turkey between 1990 and 1999. However, in Istanbul, Edirne, Canakkale, Aydin, Antalya, Mersin, Konya, Nigde, Gaziantep, Ankara, Bilecik, Karabuk, Diyarbakır, Mus, Erzincan, Sivas, Malatya, Kayseri, Kirsehir and Yozgat, the drought indicator is between 0.5 and 1. In Ardahan, Balıkesir, Mugla, Sirnak, Trabzon, Siirt and Kastamonu provinces, the SPEI drought indicator is between 0 and −0.5. Between 2000 and 2009, the drought indicator SPEI value was between 0 and 0.5 and 0–−0.5 in Turkey. However, in Istanbul, Aydin, Antalya, Malatya, Malatya, Erzincan, Nigde, Trabzon and Ardahan, the drought indicator is between 0.5 and 1. In the provinces of Sirnak, Kayseri, Mersin and Cankiri, the drought indicator was calculated to be between −0.5–−1. Between 2010 and 2019, the drought indicator SPEI value was between 0 and 0.5 and 0–−0.5 in Turkey. However, the drought indicator is between 0.5 and 1 in Istanbul, Edirne, Canakkale, Balıkesir, Aydin, Konya, Nigde, Cankiri, Diyarbakır, Kastamonu and Ankara. In Sirnak and Iğdır provinces, the drought indicator is between −0.5–−1. Between 2020 and 2029, the drought indicator SPEI value is between 0 and −0.5 in Turkey. However, it is calculated that the drought indicator value of Malatya province is between −0.5 and −1 values and the drought indicator in Sirnak province is between 0.5 and 1 values. Between the years 2030–2039, it is seen that the drought indicator SPEI value is between 0 and −0.5 values in Turkey. However, the drought indicator values of Istanbul, Canakkale, Aydin, Mugla, Nigde, Diyarbakır, Erzincan, Sivas and Ankara provinces are between −0.5–−1 values and the drought indicator in Sirnak province is between 0.5 and 1 values. Between 2040 and 2049, the drought indicator SPEI value is between 0 and −0.5 values in Turkey. However, it is concluded that the drought indicator values of Istanbul, Edirne, Canakkale, Bilecik, Aydin, Konya, Nigde, Gaziantep, Diyarbakır, Mus, Erzincan, Sivas, Ankara and Antalya are between −1.5–−1 values and the drought indicator in Sirnak is between 0.5–1 values.

Drought severity and duration vary in different time periods and regions in general. Drought conditions in major cities and agricultural production centers were observed to range from mild to moderate. Especially large cities such as Istanbul, Ankara and Antalya were significantly affected by drought conditions. Increasing drought conditions could pose serious challenges in areas such as water resources management, agricultural productivity and urbanization. This situation highlights an important need to reassess water management strategies across Turkey and to ensure the sustainability of agricultural production. Proactive measures need to be taken, taking into account the impacts of future climate change. As Turkey is under the threat of drought, many drought studies have been conducted in the region. Dabanlı et al. (2017), in their study, examined the drought analysis of Turkey by considering only precipitation data. They used 3, 6, 9 and 12-month time scales in the study. Topcu, (2022), in his study, obtained drought analyzes for different time periods between 1925 and 2016 by considering precipitation data. In his study, he evaluated drought analyzes seasonally. However, most of the drought analyzes conducted in the region only considered precipitation. However, it is known that the change in temperature plays a major role in drought formation (Ahmed et. al., 2018; Mann & Gleick, 2015). Adib and Marashi (2019) conducted drought analysis of Khuzestan province of Iran with SPI method. In their study, they concluded that the severity of drought is less in the north of Khuzestan province, while the probability of severe droughts in the central region of

Khuzestan province is less than in other regions. In addition, it has been clearly stated in studies around the world that an increase in temperature will increase evapotranspiration and lead to increased drought and therefore temperature and evaporation should be included in drought analyses (Li et. al., 2020; Lotfirad et. al., 2022; Papamichail et. al., 2001; Pei et. al., 2020; Tan et. al., 2015; Tizro et. al., 2014).

There are studies that consider precipitation and temperature in the study region. Eris et. al. (2020) evaluated the Kucuk Menderes River Basin in the Aegean region with both SPI and SPEI. They concluded that there are severe and prolonged droughts in the Kucuk Menderes River Basin. When Fig. 6 and Fig. 7 are examined, it is seen that similar results are obtained in the Kuçuk Menderes basin. Katipoglu et. al. (2020) considered Erzincan province located in the Euphrates Basin, SPI, SPEI, RDI, RAI and ZSI analyzes were applied and drought values of different methods were compared. SPEI drought values were found to be higher by using 1, 3 and 12 month time scales İn their study. When the drought values of Erzincan province in the study are compared with the results given in Fig. 6 and Fig. 7, it is seen that consistent results are obtained. As a result, the fact that 4 different time scales (3, 6, 9 and 12) were considered in this study and the drought data of the whole Turkey from 1990 to 2049 were obtained by considering precipitation and temperature values is one of the strongest aspects of this study.

4. Conclusion

In this study, a stochastic time series model was established to forecast the precipitation and temperature data of Turkey between 2020 until 2050. In the model, Seasonal Autoregressive Integrated Moving Average (SARIMA) models were used to take into account the relationship between the data and seasonality factors. In addition, the most appropriate model for each station was established separately. In the model, 90% of the data was used for training and 10% for testing. The accuracy of the predicted data was tested by correlation test (r) and Root Mean Square Error (RMSE) test. As a result of the study, the average r value for temperature data was calculated as 99% and the RMSE value as 1.46. For precipitation data, the average r value was calculated as 66% and the RMSE value as 34.6. In addition, drought models of Turkey until 2050 were established and spatial and temporal evaluation of these models were made. These models were obtained by analyzing the data of stations uniformly distributed over Turkey between 1990 and 2050 with the Standard Precipitation Evapotranspiration Index (SPEI). Different time scales (SPEI3, SPEI6, SPEI9 and SPEI12) were used in the drought analysis. In addition, spatial estimation was made using Geographic Information Systems (GIS) in order to ensure that the drought analysis covers the whole Turkey. As a result of the study, drought return interval maps of Turkey and drought maps for the years 1990–1999, 2000–2009, 2010–2019, 2020–2029, 2030–2039, 2040–2049 were created. The highlights of the study are as follows.

- According to the drought analysis of Turkey between 1990 and 2050, it is concluded that Istanbul, Edirne, Canakkale, Aydin, Antalya, Bilecik, Ankara, Konya, Nigde, Diyarbakır, Erzincan and Sivas will be in the medium arid class according to $SPEI_3$ and SPEI6 drought indicators.
- According to the $SPEI_9$ drought indicator, it is concluded that by 2050, Istanbul, Edirne, Canakkale, Aydin, Antalya, Bilecik, Ankara, Konya, Nigde, Diyarbakır, Erzincan, Sivas and Mus will be in the medium arid class according to the SPEI classification system.
- According to the $SPEI_{12}$ drought indicator, by 2050, the provinces of Istanbul, Edirne, Canakkale, Aydin, Antalya, Bilecik, Ankara, Konya, Nigde, Diyarbakır, Erzincan, Sivas, Mus, Artvin and Gaziantep will be in the medium arid class according to the SPEI classification system.
- In the maps of drought periods $SPEI_3$, $SPEI_6$, $SPEI_9$ and $SPEI_{12}$, it is seen that drought is almost in the same provinces, but the impact areas of drought have expanded.

On the other hand, in this study, the only meteorological parameters used for all models are precipitation and temperature data. The scope of the study can be extended by using other meteorological

parameters. In addition, a basin-based study instead of a province-based study would be useful in interpreting the analysis results in more detail. Addressing these issues in future studies will benefit the emergence of more comprehensive studies.

Author contribution A.I.C.: Formal Analysis, Investigation, Methodology, Resources, Software, Writing – Original Draft, Writing – Review & Editing. G.C.: Methodology, Software, Supervision, Writing – Original Draft, Writing – Review & Editing.

G.C.: Methodology, Software, Supervision, Writing – Original Draft, Writing – Review & Editing.

Funding

No funding was received from any organization for this study.

Data availability

No datasets were generated or analysed during the current study.

Declarations

Conflict of Interest The authors declare no competing interests.

Ethical Approval All authors have read, understood, and have complied as applicable with the statement on "Ethical responsibilities of Authors" as found in the Instructions for Authors and are aware.

References

Adib, A., & Marashi, S. S. (2019). Meteorological drought monitoring and preparation of long-term and short-term drought zoning maps using regional frequency analysis and L-moment in the Khuzestan province of Iran. *Theoretical and Applied Climatology, 137*, 77–87.

Aghelpour, P., Mohammadi, B., & Biazar, S. M. (2019). Long-term monthly average temperature forecasting in some climate types of Iran, using the models SARIMA, SVR, and SVR-FA. *Theoretical and Applied Climatology, 138*(3–4), 1471–1480.

Ahmed, K., Shahid, S., & Nawaz, N. (2018). Impacts of climate variability and change on seasonal drought characteristics of Pakistan. *Atmospheric Research, 214*, 364–374.

Al-Najjar, H., Ceribasi, G., Dogan, E., Abualtayef, M., Qahman, K., & Shaqfa, A. (2020). Stochastic time-series models for drought assessment in the Gaza Strip (Palestine). *Journal of Water and Climate Change, 11*(S1), 85–114.

Bates, B. C., Kundzewicz, Z. W., Wu, S., & Palutikof, J. P. (2008). *Climate Change and Water Tech Pap VI* (p. 210). Geneva: Intergovernmental Panel on Clim Change.

Blenkinsop, S., & Fowler, H. J. (2007). Changes in drought frequency, severity and duration for the British Isles projected by the PRUDENCE regional climate models. *Journal of Hydrology, 342*(1–2), 50–71.

Box, G. E. P., Jenkins, G. M., & Reinsel, G. C. (2008). *Time Series Analysis: Forecasting and Control* (4th ed.). Wiley Series in Probability and Statistics.

Box, G. E., & Jenkins, G. M. (1976). *Time series analysis: Forecasting and control San Francisco*. Holden-Day.

Chen, K. Y., & Wang, C. H. (2007). A hybrid SARIMA and support vector machines in forecasting the production values of the machinery industry in Taiwan. *Expert Systems with Applications, 32*(1), 254–264.

Dabanlı, İ, Mishra, A. K., & Şen, Z. (2017). Long-term spatio-temporal drought variability in Turkey. *Journal of Hydrology, 552*, 779–792.

Dabral, P. P., & Tabing, I. (2020). Modelling and forecasting of monthly rainfall and temperature time series using SARIMA for trend detection-a case study of Umiam, Meghalaya (India). *Int Journal of Environment and Climate Change, 10*(11), 155–172.

Djerbouai, S., & Souag-Gamane, D. (2016). Drought forecasting using neural networks, wavelet neural networks, and stochastic models: Case of the Algerois Basin in North Algeria. *Water Resources Management, 30*, 2445–2464.

Dogan, S., Berktay, A., & Singh, V. P. (2012). Comparison of multi-monthly rainfall-based drought severity indices, with application to semi-arid Konya closed basin, Turkey. *Journal of Hydrology, 470*, 255–268.

Eris, E., Cavus, Y., Aksoy, H., Burgan, H. I., Aksu, H., & Boyacioglu, H. (2020). Spatiotemporal analysis of meteorological drought over Kucuk Menderes River Basin in the Aegean Region of Turkey. *Theo. and Applied Climatology, 142*(3), 1515–1530.

Guardiola-Claramonte, M., Troch, P. A., Breshears, D. D., Huxman, T. E., Switanek, M. B., Durcik, M., & Cobb, N. S. (2011). Decreased streamflow in semi-arid basins following drought-induced tree die-off: A counter-intuitive and indirect climate impact on hydrology. *Journal of Hydrology, 406*(3–4), 225–233.

Gultepe, I., Rabin, R., Ware, R., & Pavolonis, M. (2016). Light snow precipitation and effects on weather and climate. *Advances in Geophysics* (pp. 147–210). Elsevier.

Gultepe, I., Sharman, R., Williams, P. D., Zhou, B., Ellrod, G., Minnis, P., & Neto, F. A. (2019). A review of high impact weather for aviation meteorology. *Pure and Applied Geophysics, 176*, 1869–1921.

Gumus, V. (2023). Evaluating the effect of the SPI and SPEI methods on drought monitoring over Turkey. *Journal of Hydrology, 626*, 130386.

Hamed, M. M., Sammen, S. S., Nashwan, M. S., & Shahid, S. (2023). Spatiotemporal variation of drought in Iraq for shared socioeconomic pathways. *Stochastic Environmental Research and Risk Assessment, 37*(4), 1321–1331.

Hao, Z., & Agha Kouchak, A. (2013). Multivariate standardized drought index: A parametric multi-index model. *Advances in Water Resources, 57*, 12–18.

Kam, H. J., Sung, J. O., & Park, R. W. (2010). Prediction of daily patient numbers for a regional emergency medical center using time series analysis. *Healthcare Informatics Research, 16*(3), 158–165.

Kao, S. C., & Govindaraju, R. S. (2010). A copula-based joint deficit index for droughts. *Journal of Hydrology, 380*(1–2), 121–134.

Kashyap, R. L., & Rao, A. R. (1976). Dynamic stochastic models from empirical data. *Mathematics in Science and Engineering.* Academic Press Inc.

Katipoğlu, O. M., Acar, R., & Şengül, S. (2020). Comparison of meteorological indices for drought monitoring and evaluating: A case study from Euphrates basin, Turkey. *Journal of Water and Climate Change, 11*(S1), 29–43.

Li, L., She, D., Zheng, H., Lin, P., & Yang, Z. L. (2020). Elucidating diverse drought characteristics from two meteorological drought indices (SPI and SPEI) in China. *Journal of Hydrometeorology, 21*(7), 1513–1530.

Lotfirad, M., Esmaeili-Gisavandani, H., & Adib, A. (2022). Drought monitoring and prediction using SPI, SPEI, and random forest model in various climates of Iran. *Journal of Water and Climate Change, 13*(2), 383–406.

Mann, M. E., & Gleick, P. H. (2015). Climate change and California drought in the 21st century. *Proceedings of the National Academy of Sciences, 112*(13), 3858–3859.

McKee TB, Doesken NJ, Kleist J (1993) The relationship of drought frequency and duration t time scales. In: Eighth Conference on Applied Climatology. American Meteorological Society, Anaheim

Mishra, A. K., & Singh, V. P. (2010). A review of drought concepts. *Journal of Hydrology, 391*(1–2), 202–216.

Mishra, A. K., Singh, V. P., & Desai, V. R. (2009). Drought characterization: A probabilistic approach. *Stoch Environ Res Risk Assess, 23*(1), 41–55.

Papacharalampous, G., Tyralis, H., & Koutsoyiannis, D. (2019). Comparison of stochastic and machine learning methods for multi-step ahead forecasting of hydrological processes. *Stochastic Environmental Research and Risk Assessment, 33*(2), 481–514.

Papamichail, D. M., & Georgiou, P. E. (2001). Seasonal arima inflow models for reservoir sizing 1. *JAWRA Journal of the American Water Resources Association, 37*(4), 877–885.

Paulo, A. A., & Pereira, L. S. (2008). Stochastic prediction of drought class transitions. *Water Resources Management, 22*(9), 1277–1296.

Pei, Z., Fang, S., Wang, L., & Yang, W. (2020). Comparative analysis of drought indicated by the SPI and SPEI at various timescales in inner Mongolia. *China Water, 12*(7), 1925.

Rajsekhar, D., Singh, V. P., & Mishra, A. K. (2015). Multivariate drought index: An information theory based approach for integrated drought assessment. *Journal of Hydrology, 526*, 164–182.

Şen, Z. (1998). Probabilistic formulation of spatio-temporal drought pattern. *Theoretical and Applied Climatology, 61*(3–4), 197–206.

Şen, Z. (2014). *Applied and Practical Hydrogeology* (p. 406). Elsevier.

Şen, Z. (2015). *Applied Drought Modeling, Prediction, and Mitigation* (1st ed., p. 484p). Elsevier.

Shayeghi, A., Ziveh, A. R., Bakhtar, A., Teymoori, J., Hanel, M., Godoy, M. R. V., & AghaKouchak, A. (2024). Assessing drought impacts on groundwater and agriculture in Iran using high-resolution precipitation and evapotranspiration products. *Journal of Hydrology, 631*, 130828.

Tan, C., Yang, J., & Li, M. (2015). Temporal-spatial variation of drought indicated by SPI and SPEI in Ningxia Hui Autonomous Region. *China Atmosphere, 6*(10), 1399–1421.

Thornthwaite, C. W. (1948). An approach toward a rational classification of climate. *Geographical Review, 38*(1), 55–94.

Tizro, A. T., Ghashaghaie, M., Georgiou, P., & Voudouris, K. (2014). Time Series Analysis of Water Quality Parameters. *Journal of Applied Research in Water and Wastewater, 1*, 43–52.

Topçu, E. (2022). Appraisal of seasonal drought characteristics in Turkey during 1925–2016 with the standardized precipitation index and copula approach. *Natural Hazards, 112*(1), 697–723.

Tsakiris, G., Pangalou, D., & Vangelis, H. (2007). Regional drought assessment based on the Reconnaissance Drought Index (RDI). *Water Resources Management, 21*(5), 821–833.

Vicente-Serrano, S. M., Begueria, S., & Lopez-Moreno, J. I. (2010). A multiscalar drought index sensitive to global warming: The standardized precipitation evapotranspiration index. *Journal of Climate, 23*(7), 1696–1718.

Xu, K., Yang, D., Yang, H., Li, Z., Qin, Y., & Shen, Y. (2015). Spatio-temporal variation of drought in China during 1961–2012: A climatic perspective. *Journal of Hydrology, 526*(July), 253–264.

(Received May 16, 2024, revised July 27, 2024, accepted August 8, 2024)